Macromolecules

pubs.acs.org/Macromolecules
Article

Synthesis and Morphological Analysis of Well-Defined Poly(2,6-dimethyl-1,4-phenylene ether)-*b*-Poly(dimethylsiloxane)

Riku Takahashi, Kan Hatakeyama-Sato, Yuta Nabae, and Teruaki Hayakawa*

Cite This: *Macromolecules* 2025, 58, 5271−5282
Read Online

ACCESS | Metrics & More | Article Recommendations | Supporting Information

ABSTRACT: Microphase-separated structures of block copolymers have been leveraged in advanced functional materials. However, such unique morphologies have not been extensively studied for block copolymers comprising poly(2,6-dimethyl-1,4-phenylene ether) (PPE), although PPE is a commonly utilized engineering plastic. Herein, based on precisely prepared PPE, we have developed PPE-containing block copolymers, exhibiting various microphase-separated structures such as spheres, lamellae, and cylinders. As the second block component, poly(dimethylsiloxane) (PDMS) was synthesized via living ring-opening polymerization. Block copolymers (PPE-*b*-PDMS) with different compositions were efficiently obtained by employing hydrosilylation using Karstedt's catalyst. Additionally, it was found that PPE-*b*-PDMS followed different pathways of microphase-separated structure formation depending on the solvent used for sample preparation. The developed morphologies are expected to enhance the properties of PPE through the combination with other block components and the control of nanometer-scale internal structures.

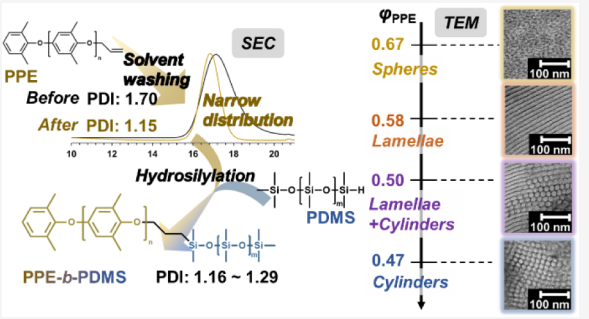

INTRODUCTION

Block copolymers consist of different polymers that are connected by chemical bonds and form self-assembled structures known as microphase-separated structures. The control and exploration of these morphologies have been studied in block copolymers composed of poly(styrene),[1,2] poly(methyl methacrylate),[3] poly(isoprene),[4] poly(2-vinylpyridine),[5,6] and poly(dimethylsiloxane).[7,8] Various microphase-separated structures, such as spheres, lamellae, cylinders, and double gyroid networks, emerge depending on the volume fraction of the constituent polymers.[9−11] These unique morphologies developed in block copolymers have been leveraged in lithography applications,[12,13] nanoporous membranes,[14,15] and functional polymer particles.[16,17]

In contrast, there are still many block copolymers for which microphase-separated structures have not been reported, even if the constituent polymers are commonly utilized. One such example is a block copolymer composed of poly(2,6-dimethyl-1,4-phenylene ether) (PPE). PPE has been used industrially as an engineering plastic. Once the PPE-containing block copolymers are developed and their microphase-separated structures are achieved, the use of PPE in a wider range of applications will be further promoted. Specifically, PPE-containing block copolymers can be applied in combination with immiscible polymers and utilized as functional materials with controlled internal structures.[18,19]

PPE-containing block copolymers have been synthesized using consecutive oxidative coupling polymerization,[20] radical polymerization,[18] and other reactions.[21−24] The synthesis of graft copolymers composed of PPE and the development of microphase-separated structures have also been reported.[19] However, to the best of our knowledge, there have been no studies that synthesized a series of PPE-containing block copolymers with different compositions and observed the alteration of various microphase-separated structures depending on the volume fraction. To address this issue, it is necessary to control the molecular weight and distribution of the constituent polymers more precisely.[9,25−27]

PPE is conventionally synthesized via oxidative coupling polymerization, resulting in uncontrolled molecular weight and broad molecular weight distribution.[28] Aiming for the controlled synthesis of PPE, refined synthetic methods have been explored in previous studies.[29,30] Nevertheless, precise control over the molecular weight and distribution has not been achieved. Thus, at present, it is difficult to precisely prepare PPE through synthetic approaches.

In this study, we aimed to create various microphase-separated structures of PPE-containing block copolymers based on precisely prepared homopolymers. PPE with controlled characteristics was obtained by meticulously

Received: March 19, 2025
Revised: April 23, 2025
Accepted: April 25, 2025
Published: May 6, 2025

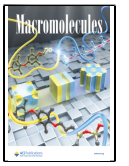

https://doi.org/10.1021/acs.macromol.5c00730
Macromolecules 2025, 58, 5271−5282

Scheme 1. Synthesis Scheme of Polymers Employed in this Study[a]

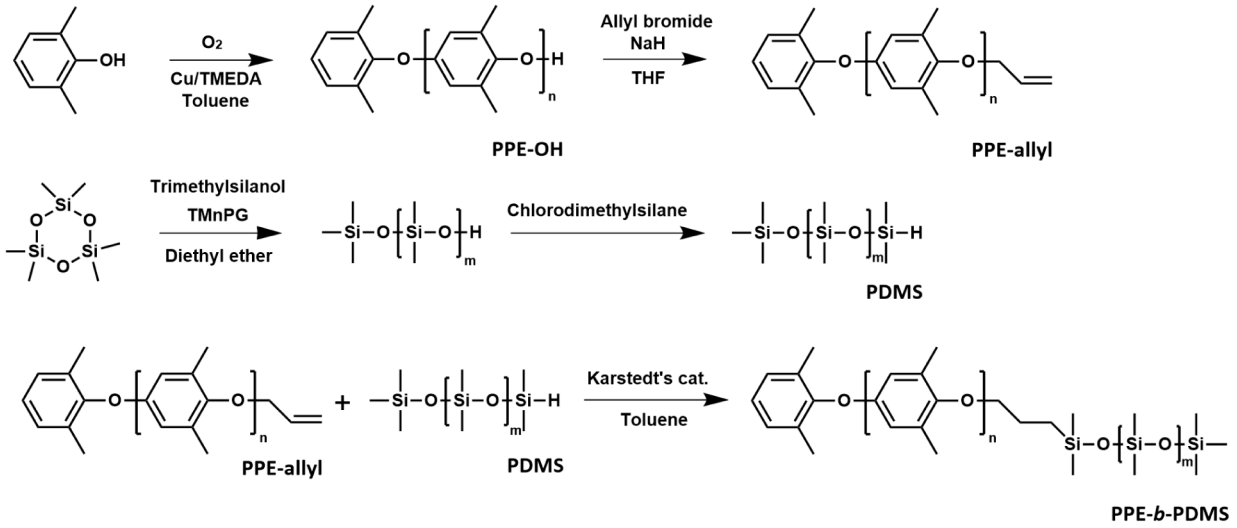

[a](1) PPE, (2) PDMS, and (3) PPE-*b*-PDMS.

extracting specific molecular weight components following oxidative coupling polymerization. Poly(dimethylsiloxane) (PDMS) was used as a second component of the block copolymer, as PDMS has a strong segregation strength with hydrocarbon polymers and is effective in promoting the microphase-separated structures.[31] PDMS was synthesized via living ring-opening polymerization and introduced onto PPE (PPE-*b*-PDMS). PPE-*b*-PDMS was synthesized through a highly efficient polymer reaction using hydrosilylation. This approach allowed for the synthesis of a series of block copolymers with varied volume fractions while maintaining the molecular weight of PPE. The developed morphologies were observed by using small-angle X-ray scattering (SAXS) and transmission electron microscopy (TEM). Various nanometer-scale ordered structures, such as spheres, lamellae, and cylinders, were achieved depending on the volume fraction of the constituent polymers. Moreover, temperature-modulated X-ray analysis was performed to further investigate the morphology of PPE-*b*-PDMS prepared from different solvents. Solubility tests and thermal analyses were also conducted for PPE-containing block copolymers.

EXPERIMENTAL SECTION

Materials. 2,6-Dimethylphenol was recrystallized twice from a heptane solution prior to use. Hexamethylcyclotrisiloxane was purified by sublimation and dissolved in diethyl ether (DEE). The DEE solution was dried over 3A molecular sieves. Trimethylsilanol was purified by distillation and dried over 3A molecular sieves. 1,3-Trimethylene-2-propylguanidine (TMnPG) was synthesized following and modifying previously reported methods. First, tetrahydropyrimidine-2-thione was synthesized from 1,3-diaminopropane and carbon disulfide.[32] Then, 2-methylthio-1,4,5,6-tetrahydropyrimidine hydroiodine was prepared from tetrahydropyrimidine-2-thione and iodomethane.[33] Finally, TMnPG was synthesized from 2-methylthio-1,4,5,6-tetrahydropyrimidine hydroiodine and propylamine.[34] Details on the synthesis of TMnPG are shown in Scheme S1 and Figures S1–S6. TMnPG was dissolved in toluene, and the solution was dried over 3A molecular sieves prior to use in the polymerization. The drying process using 3A molecular sieves mentioned above was conducted for more than 48 h.[35] Unless otherwise stated, all other chemicals were used as received.

Measurements. Nuclear magnetic resonance (NMR) spectra were recorded on a JEOL JNM-ECS 400 spectrometer at 400 MHz for ^{1}H. Size exclusion chromatography (SEC) was conducted using a ShodexGPC-101 system equipped with a ShodexLF-804 column, ShodexRI-501, and tetrahydrofuran (THF) as an eluent. Molecular weight and polydispersity index (PDI) were calculated using polystyrene (Shodex STANDARD SM-105) as a standard. Thermogravimetric analysis (TGA) was conducted using an EXSTAR TG/DTA7300 instrument at a heating rate of 10 °C min^{-1} under a nitrogen atmosphere. Differential scanning calorimetry (DSC) was conducted using an EXSTAR DSC 7020 under a nitrogen atmosphere. Small-angle X-ray scattering (SAXS) experiment was conducted at SPring-8 (Hyogo, Japan) utilizing BL-40B2 with a wavelength of 12.4 keV. Temperature-modulated SAXS measurement was performed using NANOPIX with a 1.54 Å X-ray source within the temperature range of 30−350 °C. Bright-field transmission electron microscopy (TEM) images were obtained using a Hitachi H7650 Zero.A TEM at an accelerating voltage of 100 kV. Thin-film specimens for TEM observation were prepared from samples embedded in an epoxy resin using an Ultracryotome FC-7 (Leica Microsystems) at −140 °C with a thickness setting of 80 nm. All the samples were observed without staining. In the TEM images, PPE and PDMS domains appeared as bright and dark regions, respectively.

Synthesis of PPE−OH. Poly(2,6-dimethyl-1,4-phenylene ether) with a phenolic hydroxyl group (PPE−OH) was synthesized from 2,6-dimethylphenol monomer using di-μ-hydroxo-bis[(*N*,*N*,*N*′,*N*′-tetramethylethylenediamine)-copper (II)] chloride (Cu/TMEDA) as a catalyst in a toluene/water heterogeneous system via oxidative coupling polymerization (Scheme 1).[29] The specific synthesis procedures are as follows.

Tetramethylethylenediamine (TMEDA, 0.5 mL, 3.40 mmol), H_2O (0.95 g), and Cu/TMEDA 0.215 g (0.46 mmol) were added into a test tube. Then, 2,6-dimethylphenol 10.25 g (85 mmol) in toluene 46.5 mL was added to the mixture. The solution was vigorously stirred under an oxygen atmosphere with an oxygen balloon at 50 °C for 370 min. The solution was reprecipitated in MeOH/HCl (1000 mL/5 mL) twice. Drying the remaining solid under vacuum afforded PPE−OH with lower molecular weight as a white to pale yellow solid, hereafter referred to as PPE_{47}−OH (yield: 8.75 g, 85.4%, $M_{n,\,SEC}$: 8100, and polydispersity index (PDI): 1.71). PPE−OH with a higher molecular weight (PPE_{78}−OH) was synthesized in the same manner, which is explained in the Supporting Information. The subscript number appended to "PPE" represents the degree of polymerization calculated using the molecular weight estimated from ^{1}H NMR for PPE-allyl synthesized in the subsequent reaction.

Washing Process with Solvents That Partially Dissolve PPE. To achieve PPE with a specific molecular weight, PPE−OH was

https://doi.org/10.1021/acs.macromol.5c00730
Macromolecules 2025, 58, 5271−5282

washed with organic solvents that partially dissolve PPE to remove lower molecular weight fractions by using a Soxhlet extractor. The washing process was conducted for over 24 h under air.

Synthesis of PPE-Allyl. The phenolic hydroxyl group on the PPE−OH chain end was converted into an allyl group (PPE-allyl) via a nucleophilic substitution reaction with allyl bromide (Scheme 1). Specifically, PPE_{47}−OH was converted into PPE_{47}-allyl as described below. PPE_{47}−OH (7.22 g, 0.891 mmol) and THF (70 mL) were added into a two-necked flask, and then the flask was purged with nitrogen. After adding sodium hydride (356 mg, 8.91 mmol), the solution was stirred for about 15 min. Subsequently, allyl bromide (0.713 mL, 8.91 mmol) was added to the solution, and the reaction was continued for over 24 h at room temperature. The mixture was washed with brine several times, and the product was extracted into chloroform. The chloroform solution was reprecipitated into methanol. Drying under vacuum afforded PPE_{47}-allyl with a yield of 7.14 g (99%) as a white powder. PPE_{78}−OH was converted into PPE_{78}-allyl in the same manner, as described in the Supporting Information.

Synthesis of PDMS. Hemitelechelic poly(dimethylsiloxane) (PDMS) with a hydrosilyl group on a chain end was synthesized from hexamethylcyclotrisiloxane ($D_3^{(Me2)}$) via living ring-opening polymerization (Scheme 1).[36,37] Trimethylsilanol, 1,3-trimethylene-2-propylguanidine (TMnPG) and diethyl ether (DEE) were used as the initiator, catalyst, and solvent, respectively. To end-cap the chain end, chlorodimethylsilane was used, and the chain end of the resulting PDMS was converted to a hydrosilyl group. All chemicals involved, except for chlorodimethylsilane, were dehydrated over 3A molecular sieves, as water can also act as an initiator, producing telechelic PDMS with approximately twice the molecular weight in this polymerization.[34] The specific synthesis procedure is as follows.

DEE solution of $D_3^{(Me2)}$ (1.25 mol L^{-1}) 9.00 mL (11.25 mmol) was added into a Schlenk tube under an argon atmosphere. Then, 0.051 mL of trimethylsilanol (0.45 mmol) was added to the solution. Finally, a toluene solution of TMnPG (0.625 mol L^{-1}) of 0.18 mL (0.113 mmol) was added to initiate the polymerization. After stirring for 140 min at 25 °C, chlorodimethylsilane 0.24 mL (2.2 mmol) and pyridine 0.29 mL (3.5 mmol), acting as a hydrogen chloride scavenger, were added to terminate the polymerization. The end-capping reaction was continued for over 24 h to ensure complete chain-end modification. The solution was concentrated and washed with acetonitrile several times. As a result, PDMS ($PDMS_{76}$, where the subscript number corresponds to the degree of polymerization) was obtained as a colorless viscous liquid (yield: 2.20 g, 88%, $M_{n,\,SEC}$: 7,000, $M_{n,\,NMR}$: 5,800, PDI: 1.06). PDMS with different molecular weights was synthesized using the same method by varying the ratios of the initiator to the monomer. The details are shown in the Supporting Information.

Synthesis of PPE-*b*-PDMS. A block copolymer composed of PPE and PDMS (PPE-*b*-PDMS) was synthesized from PPE-allyl and hemitelechelic PDMS via hydrosilylation using Karstedt's catalyst (platinum (0)-1,3-divinyl-1,1,3,3-tetramethyldisiloxane in xylene, Pt ∼ 2%) (Scheme 1). The specific synthesis procedure for PPE_{47}-*b*-$PDMS_{76}$ is as follows. The subscript numbers appended to "PPE" or "PDMS" represent the degrees of polymerization of PPE or PDMS calculated from ^{1}H NMR.

PPE_{47}-allyl (0.25 g, 0.044 mmol) and $PDMS_{76}$ (0.51 g, 0.088 mmol) were added into a test tube equipped with a rubber septum, and the apparatus was purged with argon. After the addition of dried toluene (5 mL) and Karstedt's catalyst (8 drops, using a 25 G injection needle), the solution was stirred at 25 °C. The progress of the reaction was traced by taking an aliquot of the solution from the reaction mixture and conducting an ^{1}H NMR measurement for the aliquot. The completion of the reaction was verified by the disappearance of the peak at 4.19 ppm derived from methylene protons adjacent to the phenolic ether group on PPE-allyl. Then, the mixture was concentrated and washed with acetone to remove residual PDMS. For PPE_{78}-*b*-$PDMS_{76}$ and PPE_{78}-*b*-$PDMS_{110}$, hexane was used as a washing solvent; when using acetone, the presence of residual PDMS was observed in ^{1}H NMR and TEM images. Drying under vacuum afforded PPE_{47}-*b*-$PDMS_{76}$ (yield: 0.316 g, 63%) as a white to pale yellow powder. PPE-*b*-PDMS with different block ratios were synthesized in the same manner, as described in the Supporting Information.

Preparation of SAXS and TEM Samples. The samples used for SAXS and TEM measurements were prepared from a solution of PPE-*b*-PDMS in chloroform and dichloromethane (5% w/w). First, the solution was filtered through a 0.25 μm PTFE membrane syringe filter. Then, the solution was slowly evaporated at 25 °C. The obtained sample was further dried under vacuum at room temperature for over 24 h. The dried sample was subsequently heat-annealed at 250 °C for 24 h as the final process. It should be noted that the annealing was conducted at approximately 50 °C higher than the glass transition temperature of PPE ($T_{g,PPE}$ is about 200 °C). The annealing temperature is well below the 5% weight loss temperature of PPE-*b*-PDMS (T_{d5} is over 350 °C). The prepared samples were used for SAXS measurement as well as TEM observation without staining. For the temperature-modulated SAXS measurement, samples before thermal annealing, which were filled into a nitrogen-purged glass capillary, were used.

Solubility Tests and Estimation of Hansen Solubility Parameters. The solubility of PPE, PDMS, and PPE-*b*-PDMS was determined by observing the appearance of each polymer solution. Samples were dissolved in solvents at a concentration of about 1 mg/mL. The solubility was classified as "soluble", "partially soluble", and "insoluble", depending on the appearance.

To evaluate the solvent affinity of PPE and PDMS, Hansen solubility parameters (δ_H) were utilized in this study.[38−40] δ_H is composed of three parameters: δ_d for nonpolar or atomic (dispersion) interactions, δ_p for dipolar interactions, and δ_h for hydrogen bonding interactions, giving δ_H as shown in eq 1.

$$\delta_H^2 = \delta_d^2 + \delta_p^2 + \delta_h^2 \quad (1)$$

The experimental method for determining δ_H of PPE and PDMS is as follows. 10 mg of the polymer sample and 10 g of solvents were taken into a vial. The mixture was stirred for over 6 h at room temperature. Subsequently, the solvent was classified as a "good" or "bad" solvent, depending on the observed solubility state. In our study, the solvent that afforded a completely homogeneous transparent solution was considered a "good" solvent. Any other solvents were classified as "bad" solvents. A total of 24 solvents listed in Table S2 were employed. δ_H values of PPE and PDMS were provided by software (HSPiP, Fourth Edition 4.1.07), processing the obtained solubility data. HSPiP software was purchased from the website (https://www.hansen-solubility.com).

RESULTS AND DISCUSSION

Synthesis of PPE and Postprocessing to Obtain PPE with a Specific Molecular Weight. Two types of PPE with a phenolic hydroxyl group on a chain end were synthesized via oxidative coupling polymerization by varying the ratios of monomer to catalyst and the reaction time (Scheme 1). One possesses a lower molecular weight (PPE_{47}−OH) and the other possesses a higher molecular weight (PPE_{78}−OH), as shown in Table 1. The subscript numbers appended to "PPE" represent the degrees of polymerization estimated from ^{1}H NMR.

Although previous studies reported on the relationship between molecular weight and the reaction conditions in oxidative coupling polymerization,[30] molecular weight control at such a high level as living polymerization methods is still challenging. Thus, in this study, to obtain PPE with a specific molecular weight, PPE−OH was washed with organic solvents that partially dissolve PPE to remove lower molecular weight fractions by using a Soxhlet extractor. Although this method is not a novel approach for controlling the characteristics of PPE,

https://doi.org/10.1021/acs.macromol.5c00730
Macromolecules 2025, 58, 5271−5282

Table 1. Characteristics of PPE with Different Molecular Weights and Washing Conditions

Sample	$M_{n,\ SEC}$ (kDa)[a]	$M_{n,\ NMR}$ (kDa)[b]	PDI[a]
PPE_{47}−OH/before washing	8.1	5.3	1.71
PPE_{47}−OH/after washing	12.0	8.1	1.25
PPE_{47}-allyl	13.7	5.7	1.32
PPE_{78}−OH/before washing	10.0	-[c]	1.70
PPE_{78}−OH/after washing	20.2	-[c]	1.15
PPE_{78}-allyl	24.2	9.4	1.20

[a]Number-average molecular weight and polydispersity index obtained from size exclusion chromatography (SEC). [b]Molecular weight calculated from ^{1}H NMR. [c]The peak corresponding to a phenolic hydroxyl group on a PPE chain-end was broad and weak, so the molecular weight was difficult to calculate.

it would be of significant value in preparing PPE with a specific molecular weight. First, the solubility of PPE−OH was investigated to find the candidates for washing solvents. PPE−OH was found to be soluble in THF, NMP, toluene, and halogenated solvents such as dichloromethane and chloroform, but insoluble in protic solvents such as methanol, ethanol, and 2-propanol. In contrast, PPE−OH was partially soluble in hexane, acetone, cyclohexane, and ethyl acetate. Based on the solubility tests, hexane, acetone, cyclohexane, and ethyl acetate, which are capable of dissolving lower molecular weight components, were selected as candidates.

Then, the effectiveness of the candidate solvents in obtaining PPE with controlled characteristics was investigated. For this experiment, PPE_{exp}−OH ($M_{n,\ SEC}$: 16,900, polydispersity index (PDI): 1.75) was utilized. Suitable solvents were determined by comparing the number-average molecular weight and PDI of PPE_{exp}−OH before and after Soxhlet washing, as provided by SEC (Figure 1 and Table 2). PPE_{exp}−OH washed with hexane showed almost the same SEC chromatogram as before washing, indicating that hexane was not suitable for removing lower molecular weight components. Subsequently, acetone was used, and it was found from the SEC chromatogram that it could remove lower molecular weight components of $M_{n\ SEC}$ 4300. Both cyclohexane and ethyl acetate were found to remove higher molecular weight components more effectively than acetone. While cyclohexane could remove components of $M_{n\ SEC}$ 8800, ethyl acetate could remove components of $M_{n\ SEC}$ 10,100, indicating that ethyl acetate is capable of removing even higher molecular weight components.

From the results of washing experiments, acetone was chosen as the washing solvent for PPE_{47}−OH to remove the components with a number-average molecular weight of around 4000. For PPE_{78}−OH, ethyl acetate was utilized to remove the components with a number-average molecular weight of around 10,000. The SEC chromatograms obtained from PPE_{47}−OH and PPE_{78}−OH before and after washing are shown in Figure 2. Lower molecular weight components were removed after washing with solvents. The PDI changed from 1.71 to 1.25 for PPE_{47}−OH, and from 1.70 to 1.15 for PPE_{78}−OH after washing with solvents (Table 1).

A phenolic hydroxyl group on a chain end was converted to an allyl group, affording PPE-allyl. ^{1}H NMR spectra before and after allylation are shown in Figures S7−S10. Characteristics of PPE before and after allylation are shown in Table 1. Significant changes in the SEC chromatograms were not observed after allylation (Figures S11 and S12). The slight changes in $M_{n,\ SEC}$ and PDI observed after the allylation are

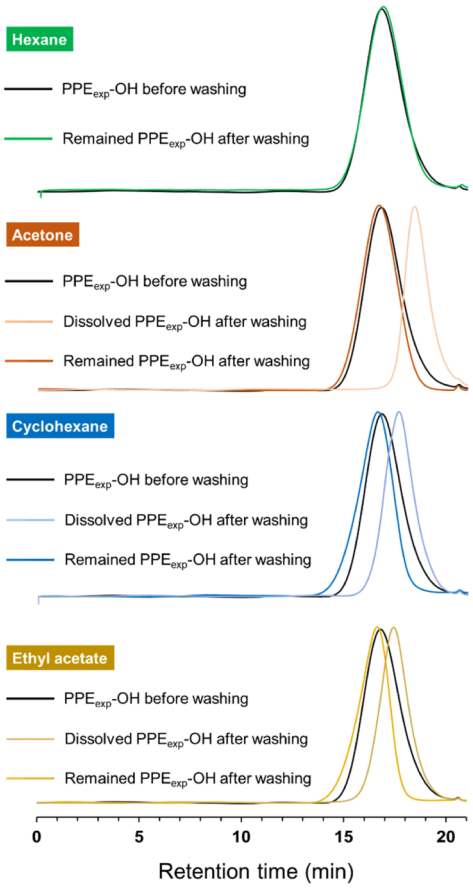

Figure 1. SEC chromatograms of PPE_{exp}−OH before and after washing with hexane (green), acetone (orange), cyclohexane (blue), and ethyl acetate (yellow). Based on these results, acetone and ethyl acetate were determined to be the appropriate washing solvents for PPE_{47}−OH and PPE_{78}−OH, respectively.

Table 2. Characteristics of PPE_{exp}−OH Before and After Washing with Solvents

Sample	$M_{n,\ SEC}$ (kDa)[a]	PDI[a]
PPE_{exp}−OH/before washing	16.9	1.75
Remained PPE_{exp}−OH/after washing with hexane[b,c]	15.6	1.69
Remained PPE_{exp}−OH/after washing with acetone[b]	20.0	1.60
Dissolved PPE_{exp}−OH/after washing with acetone[d]	4.3	1.39
Remained PPE_{exp}−OH/after washing with cyclohexane[b]	24.4	1.60
Dissolved PPE_{exp}−OH/after washing with cyclohexane[d]	8.8	1.49
Remained PPE_{exp}−OH/after washing with ethyl acetate[b]	26.8	1.47
Dissolved PPE_{exp}−OH/after washing with ethyl acetate[d]	10.1	1.51

[a]Number-average molecular weight and polydispersity obtained from size exclusion chromatography (SEC). [b]PPE_{exp}−OH insoluble in the solvents. [c]When washing with hexane, a sufficient amount of dissolved PPE_{exp}−OH was not obtained for SEC measurement. [d]PPE_{exp}−OH soluble in the solvents.

considered to originate from the transformation of the PPE terminal functional groups. It has been previously reported that changes in the functional groups alter the polymer size in the eluent, leading to variations in $M_{n,\ SEC}$ and PDI.[41] The resulting

https://doi.org/10.1021/acs.macromol.5c00730
Macromolecules 2025, 58, 5271−5282

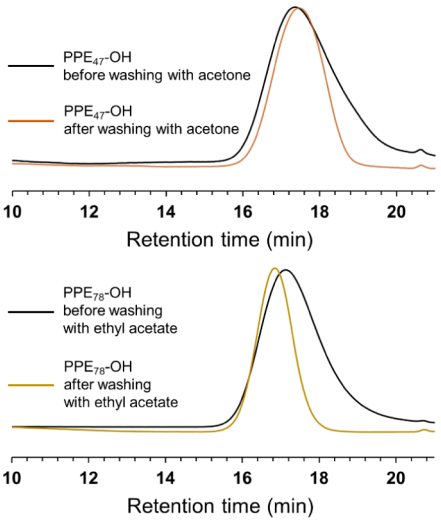

Figure 2. SEC chromatograms of PPE−OH with lower (PPE_{47}−OH) and higher (PPE_{78}−OH) molecular weights before and after washing with solvents.

PPE_{47}-allyl (M_n: 5,700, PDI: 1.32) and PPE_{78}-allyl (M_n: 9,400, PDI: 1.20) possessed lower PDI compared with as-synthesized PPE_{47}−OH (PDI: 1.71) and PPE_{78}−OH (PDI: 1.70). These PPE-allyl samples with low PDI were used in the synthesis of PPE-*b*-PDMS.

Synthesis of PDMS. PDMS with different molecular weights, possessing a hydrosilyl group on a chain end, were synthesized via ring-opening polymerization using TMnPG as a catalyst. The molecular weight was controlled by modifying the ratio of the initiator to the monomer, as explained in the Supporting Information. The PDMS synthesized and employed in this study are $PDMS_{32}$, $PDMS_{48}$, $PDMS_{67}$, $PDMS_{76}$, and $PDMS_{110}$, as listed in Table S1. The subscript numbers appended to "PDMS" represent the degrees of polymerization. ^{1}H NMR spectra of PDMS are shown in Figures S13−S17.

All of the PDMS, except for $PDMS_{110}$, showed an almost unimodal SEC chromatogram (Figure S18). On the other hand, $PDMS_{110}$ showed an SEC chromatogram with a slight shoulder peak at an earlier retention time. The higher molecular weight component, which emerged at an earlier retention time, is predicted to originate from PDMS initiated by water or from the dimerization of propagating PDMS chains, which tends to occur in the late stage of polymerization.[34,36] Figure S19 shows the SEC chromatograms of PDMS synthesized using dehydrated ($PDMS_{76}$) and non-dehydrated catalyst (PDMS_A). In PDMS_A, a shoulder peak estimated to be derived from PDMS initiated by water was observed. On the other hand, when using a dehydrated catalyst, no such shoulder peak was observed, suggesting that water contamination was almost restricted. All PDMS in this study were synthesized under the same conditions as $PDMS_{76}$, except for the ratio of initiator to monomer. Therefore, the shoulder peak observed in $PDMS_{110}$ was presumably attributed to dimerization and not the initiation by water. We considered that the undesired larger molecular weight component would not be involved in the synthesis of the block copolymer, as both chain ends of the dimerization product were trimethylsilyl groups (Figure S20). All of the synthesized polymers were employed in the synthesis of PPE-*b*-PDMS.

Synthesis of PPE-*b*-PDMS. PPE-*b*-PDMS with different block ratios were synthesized from PPE-allyl and an excessive amount of PDMS via the reaction between the allyl group on the PPE chain-end and the hydrosilyl group on the PDMS chain-end (Scheme 1). Two varieties of PPE (PPE_{47}-allyl and PPE_{78}-allyl) and five types of PDMS ($PDMS_{32}$, $PDMS_{48}$, $PDMS_{67}$, $PDMS_{76}$, and $PDMS_{110}$) were used to create six different PPE-*b*-PDMS. The subscript numbers denote the degrees of polymerization. The synthesized PPE-*b*-PDMS was washed with acetone or hexane to remove residual PDMS. ^{1}H NMR spectra of PPE-*b*-PDMS revealed that it contained little or no PPE and PDMS homopolymer residues, as evidenced by the absence of peaks derived from the chain-end of PPE-allyl (4.19, 5.19, 5.38, and 6.08 ppm) and the PDMS chain-end (4.64 ppm) (Figures 3 and S21−S25). The synthesis of PPE-*b*-

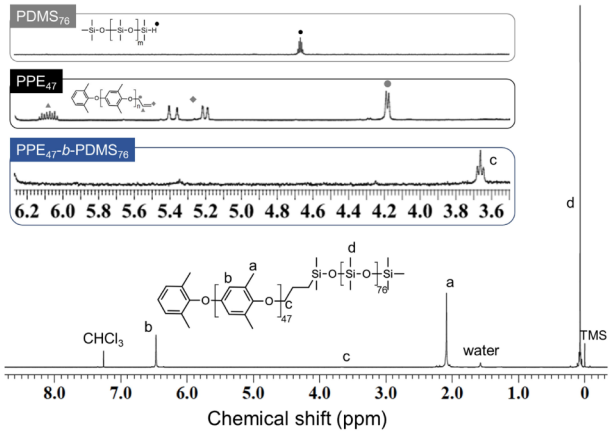

Figure 3. ^{1}H NMR spectrum of PPE_{47}-*b*-$PDMS_{76}$, exhibiting that PPE_{47}-*b*-$PDMS_{76}$ did not contain PDMS or PPE homopolymers. The enlarged view of PPE_{47}-*b*-$PDMS_{76}$ spectrum from 3.5 to 6.3 ppm is surrounded by a blue square. ^{1}H NMR spectra of $PDMS_{76}$ and PPE_{47} in the same chemical shift region are surrounded by gray and black squares, where peaks are characterized by gray or black circles, triangles, and rhombuses.

PDMS was verified by a triplet peak at 3.67 ppm corresponding to a methylene group adjacent to a phenylene ether group (marked with "c" in Figure 3). The progress of the reaction was also confirmed by an SEC chromatogram with a peak at a retention time earlier than that of PDMS or PPE homopolymers (Figure 4). Overlaid SEC chromatograms in Figure 4 also revealed that PPE-*b*-PDMS was almost separated from PPE and PDMS components. Characteristics of PPE-*b*-PDMS synthesized in this study are listed in Table 3. The volume fractions of PPE (φ_{PPE}) ranged from 0.47 to 0.67, and PDI ranged from 1.16 to 1.29. PDI values observed in this study were significantly lower than those of previously reported PPE-containing block copolymers.[18,22]

Solubility of PPE-*b*-PDMS. To examine the fundamental chemical properties and processability, we investigated the solubility of PPE, PDMS, and PPE-*b*-PDMS in common organic solvents. PPE (PPE_{47}-allyl) and PDMS (M_n: 5700, PDI: 1.09) were utilized in this experiment. Two types of PPE-*b*-PDMS with the lowest volume fraction of PPE (PPE_{47}-*b*-$PDMS_{32}$) and another with a higher volume fraction of PPE (PPE_{47}-*b*-$PDMS_{67}$) were examined. After stirring the solution for over 1 h, the solubility was determined depending on the appearance. The observed solubility was classified into "soluble" (the solution was transparent, and no residual solid was observed), "partially soluble" (the solution was slightly turbid, or a small amount of residue was observed), and

https://doi.org/10.1021/acs.macromol.5c00730
Macromolecules 2025, 58, 5271−5282

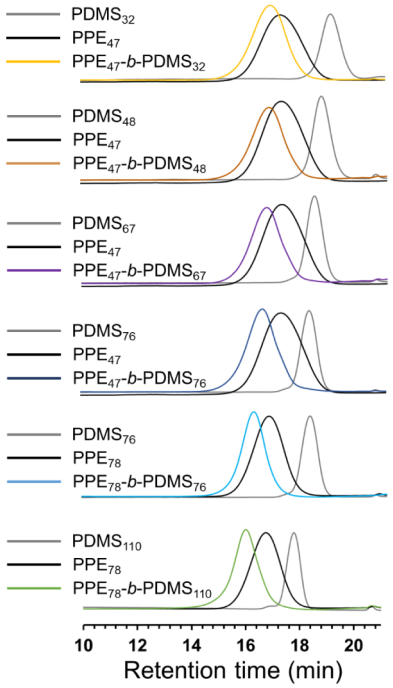

Figure 4. Overlayed SEC chromatograms of PPE, PDMS, and PPE-*b*-PDMS.

"insoluble" (the solution was turbid, or residue was observed). The results of the solubility tests are listed in Table 4, where + +, +, and − denote the solubility levels of "soluble", "partially soluble", and "insoluble", respectively. PPE-*b*-PDMS was soluble in chloroform, dichloromethane, pyridine, THF, and toluene, and insoluble in acetone, 1,4-dioxane, ethyl acetate, NMP, DMF, and 2-propanol. Acetone, 1,4-dioxane, ethyl acetate, and 2-propanol dissolve PDMS well, but PPE-*b*-PDMS strongly reflects the properties of PPE, making PPE-*b*-PDMS insoluble in these solvents. On the other hand, PPE-*b*-PDMS exhibited different solubility in cyclohexane, diethyl ether, and hexane, depending on the composition. For PPE_{47}-*b*-$PDMS_{67}$, the characteristics of PDMS were reflected due to a higher PDMS composition, resulting in the slight solubility of PPE-*b*-PDMS. However, insolubility was observed for PPE_{47}-*b*-$PDMS_{32}$, as the PDMS content was lower.

Thermal Analyses of PPE-*b*-PDMS. Thermal properties were evaluated via thermogravimetric analysis (TGA) and differential scanning calorimetry (DSC) for PPE, PDMS, and PPE-*b*-PDMS. First, heat resistance measured via TGA (at a heating rate of 10 °C min^{-1} from 30 to 550 °C under a nitrogen atmosphere) is discussed. PPE_{47}, $PDMS_{32}$, which were utilized to synthesize PPE-*b*-PDMS, and a series of PPE-*b*-PDMS with different compositions were employed for this experiment. PPE_{77} ($M_{n,\ NMR}$: 9.2 kDa, PDI: 1.24) with nearly the same characteristics as PPE_{78} was also employed herein. Figure 5 shows the results of TGA, and the temperatures of 5% weight loss (T_{d5}) are also listed in Table 3. PPE_{47} and $PDMS_{32}$ homopolymers exhibited T_{d5} values of 427 and 345 °C, respectively. Observed T_{d5} for PPE_{47} is higher than those of polystyrene (T_{d10}: 384 °C, heating rate of 10 °C/min),[42] poly(methyl methacrylate) (T_{d10}: 213 °C, heating rate of 20 °C/min),[43] poly(butadiene) (T_{d10}: around 400 °C, heating rate of 10 °C/min),[44] poly(2-vinylpyridine) (T_{d10}: around 350 °C, heating rate of 10 °C/min),[45] and poly(4-vinylpyridine) (T_{d10}: around 340 °C, heating rate of 10 °C/min),[45] which have been conventionally utilized to synthesize block copolymers for morphological analysis. All of the analyses mentioned above were conducted under a nitrogen atmosphere. It is expected that block copolymers containing PPE with superior thermal properties can be synthesized due to the higher thermal stability of PPE. In this study, PPE-*b*-PDMS synthesized from PPE_{47} exhibited T_{d5} of over 400 °C, and

Table 4. Solubility of PPE, PDMS, and PPE-*b*-PDMS in Common Organic Solvents at Room Temperature[a]

Solvent	PPE	PDMS	PPE_{47}-*b*-$PDMS_{32}$	PPE_{47}-*b*-$PDMS_{67}$
Acetone	−	++	−	−
Chloroform	++	++	++	++
Cyclohexane	+	++	−	+
Dichloromethane	++	++	++	++
Diethyl ether	−	++	−	+
1,4-Dioxane	−	++	−	−
Ethyl acetate	−	++	−	−
Hexane	−	++	−	+
NMP[b]	+	−	−	−
DMF[b]	−	−	−	−
2-Propanol	−	++	−	−
Pyridine	++	−	++	++
THF[b]	++	++	++	++
Toluene	++	++	++	++

[a]The symbols ++, +, and − represent solubility levels as "soluble", "partially soluble", and "insoluble", respectively. [b]NMP, DMF, and THF represent 1-methyl-2-pyrrolidone, *N*,*N*-dimethylformamide, and tetrahydrofuran, respectively.

Table 3. Characteristics of a Series of PPE-*b*-PDMS Synthesized via Hydrosilylation

Sample	$M_{n,\ NMR}$ (kDa)[a]	$M_{n,\ SEC}$ (kDa)[b]	PDI[b]	φ_{PPE}[c]	T_{d5} (°C)[d]	T_g (°C)[e]	Morphology[f]	*d* (nm)[g]
PPE_{47}-*b*-$PDMS_{32}$	10.8	20.4	1.29	0.67	404	192	Spheres	17.0
PPE_{47}-*b*-$PDMS_{48}$	14.0	21.8	1.28	0.58	414	194	Lamellae	20.6
PPE_{47}-*b*-$PDMS_{67}$	16.5	23.2	1.25	0.50	413	204	Lamellae	20.4 (Lamellae)
							Cylinders	25.3 (Cylinders)
PPE_{47}-*b*-$PDMS_{76}$	15.4	25.4	1.29	0.47	405	193	Cylinders	25.6
PPE_{78}-*b*-$PDMS_{76}$	20.8	34.7	1.16	0.59	366	207	Lamellae	25.8
PPE_{78}-*b*-$PDMS_{110}$	26.2	39.5	1.24	0.51	359	209	Lamellae	33.1

[a]Molecular weight calculated from ^{1}H NMR of the synthesized PPE-*b*-PDMS. [b]Number-average molecular weight and polydispersity obtained using size exclusion chromatography (SEC). [c]Volume fraction of PPE estimated based on the weight ratio of PPE and the density of PPE and PDMS. The weight ratio of PPE was calculated based on the molecular weight of PPE and PDMS homopolymers. The details are shown in the Supporting Information. [d]Temperature of 5% weight loss measured by TGA. [e]Glass transition temperature determined by DSC. [f]Determined by SAXS and TEM. [g]*d*-Spacing determined from SAXS.

https://doi.org/10.1021/acs.macromol.5c00730
Macromolecules 2025, 58, 5271−5282

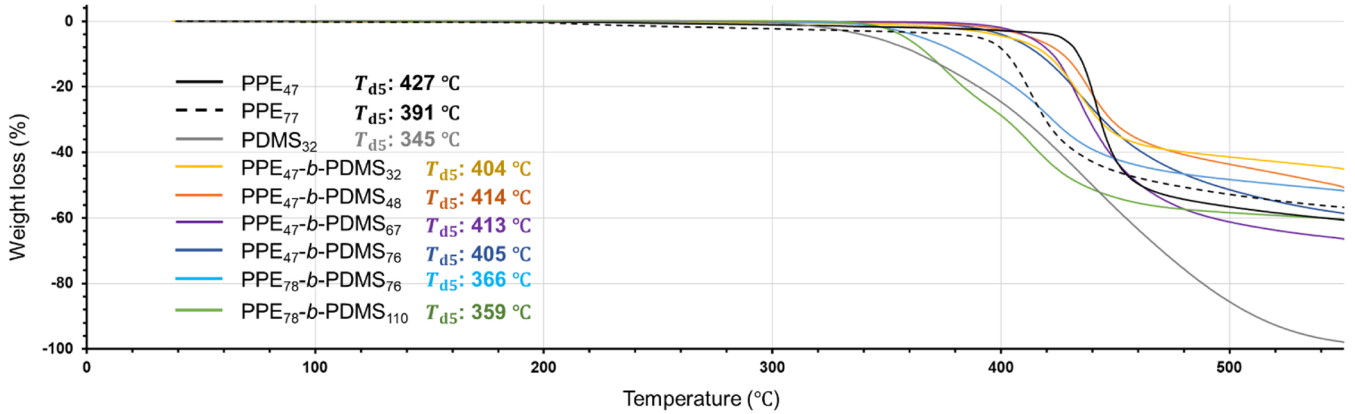

Figure 5. Thermogravimetric analysis (TGA) results for PPE, PDMS, and PPE-*b*-PDMS.

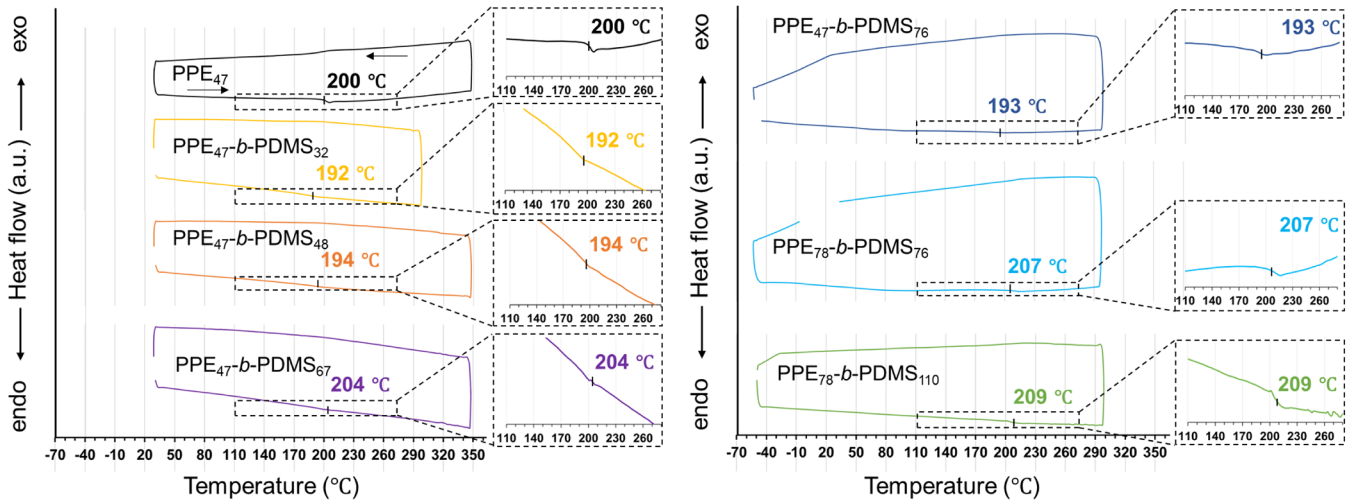

Figure 6. Differential scanning calorimetry (DSC) curves obtained from PPE and PPE-*b*-PDMS. Enlarged views of the temperature range from 110 to 280 °C around the glass transition temperatures are surrounded by dotted squares.

there was no observed trend of decreasing temperature of weight loss with higher content of PDMS, which exhibited lower T_{d5} than PPE. However, PPE-*b*-PDMS composed of PPE_{78} exhibited T_{d5} of around 360 °C, approximately 40 °C lower than those composed of PPE_{47}. At this stage, the reason for the lower T_{d5} exhibited by PPE_{78}-*b*-$PDMS_{76}$ and PPE_{78}-*b*-$PDMS_{110}$ is not yet clear; however, PPE_{77} with nearly the same molecular weight as PPE_{78} also showed lower T_{d5} compared with PPE_{47}.

PPE_{47} and a series of PPE-*b*-PDMS were also analyzed by differential scanning calorimetry (DSC). DSC curves in the second scan obtained from PPE_{47} and PPE-*b*-PDMS are shown in Figure 6. The glass transition of PPE_{47} was observed at 200 °C, consistent with previously reported values.[28] In PPE-*b*-PDMS, glass transitions derived from the PPE component were detected around 200 °C. These results suggest phase separation between PPE and PDMS domains. The glass transition of each component is observed at a different temperature from that of the homopolymer when the two components are not separated. The glass transition of PDMS, which is reported to be detected around −120 °C,[46] was not observed within the temperature range examined in this study.

Morphological Analysis of PPE-*b*-PDMS. Morphologies of PPE-*b*-PDMS bulk samples were investigated via SAXS and TEM. Samples discussed in this section were prepared from either a chloroform solution or a dichloromethane solution. The samples were subsequently annealed at 250 °C for 24 h, which is sufficiently higher than the glass transition temperatures of PPE and PDMS. TEM observation was conducted without staining. PPE and PDMS domains appeared as bright and dark regions in the TEM images. SAXS profiles and TEM images of PPE-*b*-PDMS synthesized from PPE_{47} are shown in Figure 7. The solvent following the sample name corresponds to the solvent used for sample preparation. For PPE_{47}-*b*-$PDMS_{32}$_$CHCl_3$, which possesses a volume fraction of PPE (φ_{PPE}) of 0.67, a clear ordered structure was not observed, but a vague phase separation of spherical PDMS domains in the PPE matrix can be seen in a TEM image. The SAXS profile showed a sharp peak marked with a white arrow and a broad peak marked with a black arrow. These peaks are speculated to correspond to interparticle interference of the spherical microdomains, and the scattering from isolated spherical microdomains, respectively.[4] From the TEM and SAXS analyses, spherical microphase separation is speculated to be possible in PPE_{47}-*b*-$PDMS_{32}$. This behavior deviates from the phase diagram of the typical microphase-separated structure of diblock copolymers, where cylinders are stable at a volume fraction of around 0.67.[9] One of the factors contributing to this deviation is a relatively large polydispersity index (PDI) of PPE. The effect of PDI on the microphase-separated structure

https://doi.org/10.1021/acs.macromol.5c00730
Macromolecules 2025, 58, 5271−5282

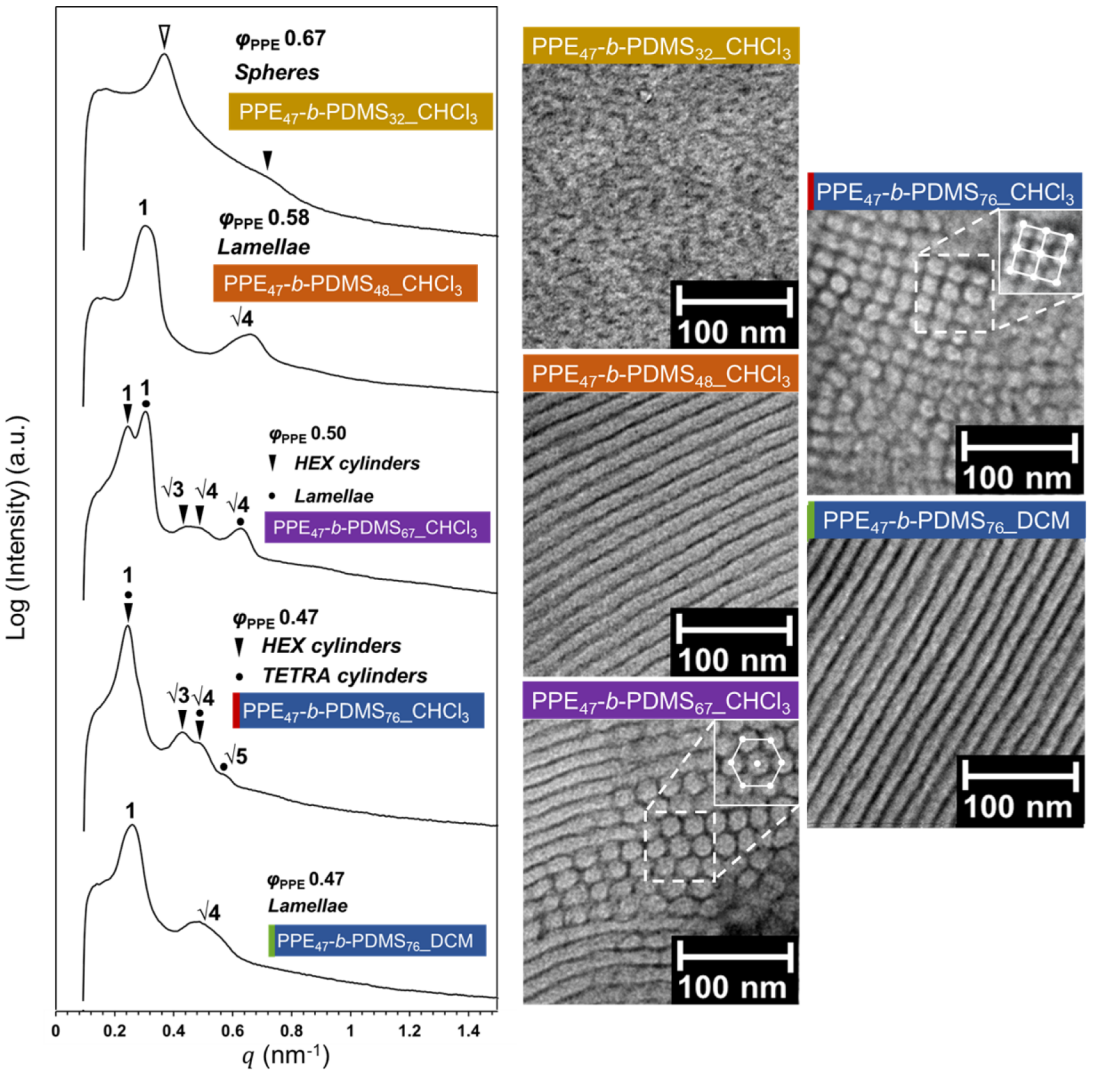

Figure 7. SAXS profiles and TEM images of PPE-*b*-PDMS composed of PPE_{47}. Solvents used for sample preparation are given by the sample name. Bright and dark regions are the PPE and PDMS domains, respectively.

has been studied based on self-consistent field theory (SCFT), and it has been shown that the phase diagram changes with an increase in the PDI of the constituent polymers.[25] However, a block copolymer composed of a polymer with a PDI of 1.2, which is close to that of PPE-*b*-PDMS, is reported to exhibit a phase diagram similar to that of a system, where the influence of PDI is negligible. Therefore, in the case of PPE-*b*-PDMS, in addition to PDI, the conformational asymmetry of the constituent polymers is also considered to affect the microphase-separated structure. The effect of conformational asymmetry on the phase diagram has also been investigated through SCFT calculations.[47,48] PPE contains aromatic rings in its main chain, resulting in low flexibility, whereas PDMS, composed of Si−O bonds, is highly flexible and can adopt various conformations, presumably leading to the conformational asymmetry of PPE-*b*-PDMS.

PPE_{47}-*b*-$PDMS_{48}$_$CHCl_3$ exhibited clear lamellar microdomains in a TEM image, verified by peaks at the relative positions of 1 and $\sqrt{4}$, in the SAXS profile. Compared with PPE_{47}-*b*-$PDMS_{32}$_$CHCl_3$, a larger φ_{PPE} value led to a morphological change from spheres to lamellae, following a general microphase separation phase diagram.[9]

For PPE_{47}-*b*-$PDMS_{67}$_$CHCl_3$, both cylindrical and lamellar microdomains were observed. In the TEM image, the coexistence of lamellar structures and circular cross-sections of hexagonally packed cylinders can be seen. The SAXS profile also indicated the coexistence of lamellae (relative peak positions at 1, $\sqrt{4}$, marked with dots) and hexagonally packed cylinders (relative peak positions at 1, $\sqrt{3}$, and $\sqrt{4}$, marked with triangles). The SAXS profile revealed different *d*-spacings for lamellae and cylinders. The volume fraction (φ_{PPE} = 0.50) is considered to be around the boundary between the volume fractions, where lamellae and cylinders are formed.

In PPE_{47}-*b*-$PDMS_{76}$_$CHCl_3$, with an even higher φ_{PPE}, cylindrical microdomains were observed. Interestingly, the emergence of tetragonally packed cylinders, in addition to hexagonally packed cylinders, can be seen in a TEM image. This was confirmed by the peaks at the relative positions of 1, $\sqrt{4}$, and $\sqrt{5}$, marked with dots in the SAXS profile: $\sqrt{5}$ peak is characteristic of tetragonally packed cylinders. The SAXS profile also indicated the emergence of hexagonally packed cylinders at the relative peak positions of 1, $\sqrt{3}$, and $\sqrt{4}$. In previous studies, tetragonally packed cylinders were observed in comb−coil block copolymers[49,50] and binary block copolymer blend systems.[51−53] In these studies, the formation

https://doi.org/10.1021/acs.macromol.5c00730
Macromolecules 2025, 58, 5271−5282

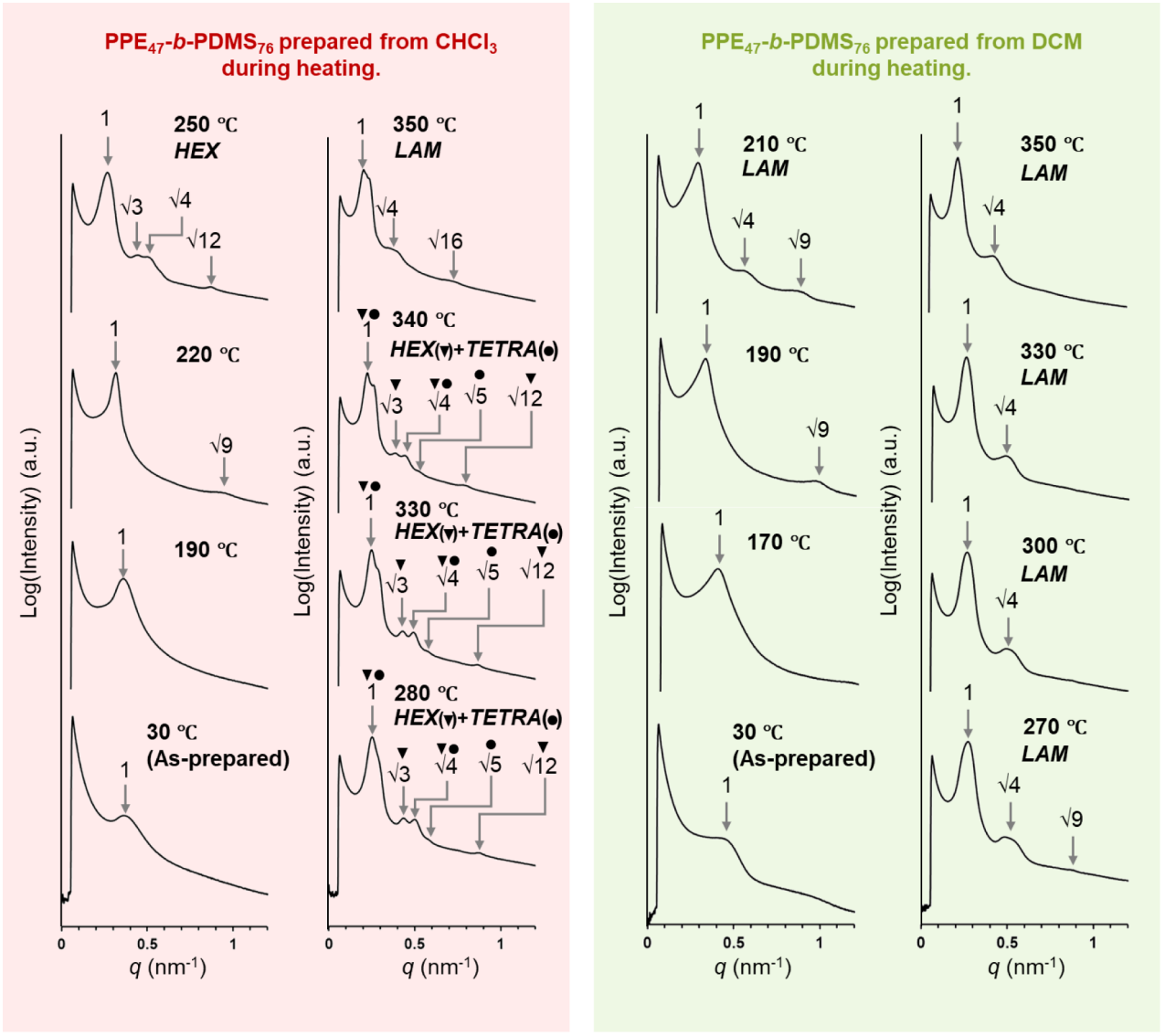

Figure 8. SAXS profiles of PPE_{47}-*b*-$PDMS_{76}$ prepared from chloroform ($CHCl_3$) and dichloromethane (DCM) at different temperatures during heating. HEX, TETRA, and LAM represent hexagonally packed cylinders, tetragonally packed cylinders, and lamellae.

of tetragonally packed cylinders was explained by the contraction of matrix polymer chains based on the orientation of the lamellar structures organized by the comb block,[49,50] or the contraction of polymer chains through hydrogen bonding.[51] In our study, the mechanism of the development of tetragonally packed cylinders is still unclear, but it is assumed that the combination of rigid (PPE) and flexible (PDMS) polymers is related to the formation. Since PPE is rigid and lacks flexibility, it presumably avoided dense packing and formed tetragonally packed cylinders, which possess a lower density of packing.

In contrast, PPE_{47}-*b*-$PDMS_{76}$_DCM exhibited a lamellar morphology in the SAXS profile and the TEM image. These results indicate that, despite thermal annealing at a temperature sufficiently higher than the glass transition temperature after solvent casting, morphologies dependent on the solvent were formed in PPE_{47}-*b*-$PDMS_{76}$. The reason for the solvent-dependent morphologies will be discussed in the next section.

PPE-*b*-PDMS composed of PPE_{78} also exhibited clear microphase-separated structures (Figure S26). The development of lamellae with a larger *d*-spacing compared to PPE-*b*-PDMS comprising PPE_{47} was verified by SAXS and TEM for both PPE_{78}-*b*-$PDMS_{76}$_$CHCl_3$ (φ_{PPE} = 0.59) and PPE_{78}-*b*-$PDMS_{110}$_$CHCl_3$ (φ_{PPE} = 0.51). In PPE-*b*-PDMS composed of PPE_{47}, the coexistence of lamellae and cylinders was observed at the φ_{PPE} of 0.50, whereas in PPE-*b*-PDMS composed of PPE_{78}, lamellae were observed at a similar volume fraction (φ_{PPE} = 0.51), suggesting that lamellae are formed over a wider composition range as a result of a larger total number of segments.

Temperature-Modulated SAXS Analysis of PPE_{47}-*b*-$PDMS_{76}$. In PPE_{47}-*b*-$PDMS_{76}$, lamellar and cylindrical morphologies were observed depending on the solvent used for sample preparation, even after thermal annealing at 250 °C, which is sufficiently higher than the glass transition temperature of PPE. To investigate this behavior, temperature-modulated SAXS measurements were conducted for PPE_{47}-*b*-$PDMS_{76}$ samples prepared from chloroform ($CHCl_3$) and dichloromethane (DCM) within the temperature range of 30−350 °C. The maximum temperature of 350 °C is approximately 50 °C lower than T_{ds} of PPE_{47}-*b*-$PDMS_{76}$. The results of the heating process are shown in Figure 8. For both solvents, only

https://doi.org/10.1021/acs.macromol.5c00730
Macromolecules 2025, 58, 5271−5282

the first-order peak was observed in the SAXS profile of the as-prepared sample (30 °C), suggesting the formation of a disordered microphase-separated structure. The disordered microphase separation was maintained up to approximately 170−190 °C. Subsequently, a well-defined microphase-separated structure began to form in the temperature range of 190−220 °C. This temperature range corresponds to the glass transition temperature of PPE. At even higher temperatures, different phase behaviors were observed for each sample. For the sample prepared from DCM, lamellae were observed around 210 °C, and the structure was maintained up to 350 °C. In contrast, for the $CHCl_3$ sample, cylindrical structures were observed around 250 °C. At first, only hexagonally packed cylinders were observed, but at 280 °C, the formation of tetragonally packed cylinders began to be observed as well. The cylinders were maintained up to 340 °C, but at 350 °C, a transition to lamellae was observed. During the cooling process, the lamellar structure was maintained down to 30 °C for both samples (Figure S27).

This result suggests that the structural formation process depends on the solvent affinity for PPE and PDMS. The solvent affinity was estimated by utilizing Hansen solubility parameters (δ_H) (Tables S2 and S3). A larger value of $\sqrt{(\delta_{H,Polymer} - \delta_{H,Solvent})^2}$ indicates a smaller affinity between a polymer and a solvent, whereas a smaller value indicates a larger affinity. Table S3 indicates that $CHCl_3$ possesses a higher affinity for PDMS, while DCM has approximately equal affinity for both PPE and PDMS. In the case of $CHCl_3$, its higher affinity for PDMS caused a larger volume fraction of PDMS in the as-prepared sample. The apparent increase in the volume fraction of PDMS (decrease in φ_{PPE} value) induced by the solvent affinity is presumed to promote the formation of cylindrical structures with PDMS as a matrix. Conversely, since DCM has an equal affinity for both PPE and PDMS, the apparent volume fraction of the as-prepared sample was almost equal to the actual volume fraction (φ_{PPE} = 0.47). Therefore, it is considered that lamellar structures were formed upon heating. The observation of a transition from cylinders to lamellae at 350 °C further suggests that the lamellar structure would be thermodynamically more stable than the cylindrical structure for PPE_{47}-*b*-$PDMS_{76}$ prepared from $CHCl_3$.

In summary, the solvent-dependent morphology observed in PPE_{47}-*b*-$PDMS_{76}$, despite thermal annealing at 250 °C—50 °C higher than the glass transition temperature—can be explained by the following two factors. First, the microphase separation process differs when using $CHCl_3$ and DCM. Second, reaching a thermodynamically stable structure of PPE_{47}-*b*-$PDMS_{76}$ requires an even higher annealing temperature.

CONCLUSION

We selectively extracted PPE with a specific molecular weight through a convenient solvent washing process. By employing PDMS with controlled characteristics and a highly efficient hydrosilylation, we precisely obtained a series of PPE-*b*-PDMS. Meticulously prepared PPE-*b*-PDMS exhibited alterations in the microphase-separated structures, transitioning from spheres to cylinders depending on the volume fraction of PPE (φ_{PPE}). It was also found that PPE-*b*-PDMS underwent different microphase separation pathways, depending on the solvents used for sample preparation. The observed morphologies, as well as the synthetic method described in this study, can be applied to the further development of PPE-based materials, such as PPE-containing block copolymers and materials with internally controlled nanometer-scale structures.

ASSOCIATED CONTENT

Supporting Information

The Supporting Information is available free of charge at https://pubs.acs.org/doi/10.1021/acs.macromol.5c00730.

Synthetic procedures of TMnPG, PPE−OH, PPE-allyl, PDMS, and PPE-*b*-PDMS, ^{1}H NMR spectra, ^{13}C NMR spectra, and SEC chromatograms of the synthesized materials, the procedure to determine the volume fraction of PPE, SAXS profiles and TEM images of PPE_{78}-*b*-$PDMS_{76}$ and PPE_{78}-*b*-$PDMS_{110}$, temperature-modulated SAXS profiles of PPE_{47}-*b*-$PDMS_{76}$ during the cooling process, a list of solvents used to estimate Hansen solubility parameters, and the estimated Hansen solubility parameters of PPE and PDMS (PDF)

AUTHOR INFORMATION

Corresponding Author

Teruaki Hayakawa − *Department of Materials Science and Engineering, Institute of Science Tokyo, Meguro-ku, Tokyo 152-8552, Japan*; orcid.org/0000-0002-1704-5841; Phone: +81-3-5734-2421; Email: hayakawa.t.ac@m.titech.ac.jp

Authors

Riku Takahashi − *Department of Materials Science and Engineering, Institute of Science Tokyo, Meguro-ku, Tokyo 152-8552, Japan*; orcid.org/0009-0008-7266-0493

Kan Hatakeyama-Sato − *Department of Materials Science and Engineering, Institute of Science Tokyo, Meguro-ku, Tokyo 152-8552, Japan*

Yuta Nabae − *Department of Materials Science and Engineering, Institute of Science Tokyo, Meguro-ku, Tokyo 152-8552, Japan*; orcid.org/0000-0002-9845-382X

Complete contact information is available at: https://pubs.acs.org/10.1021/acs.macromol.5c00730

Notes

The authors declare no competing financial interest.

ACKNOWLEDGMENTS

The authors sincerely thank Prof. Tomoyasu Hirai (Osaka Institute of Technology) and Dr. Noboru Ohta (Japan Synchrotron Radiation Research Institute (JASRI)) for their kind help with SAXS measurements at BL40B2 of SPring-8 with the approval of JASRI (Proposal Nos. 2023A1197, 2023B1112, and 2024B1228). We also sincerely thank Mr. Ryohei Kikuchi (Materials Analysis Division, Core Facility Center, Institute of Science Tokyo) for his kind support with the TEM measurements. Additionally, we deeply thank Dr. Takashi Kajitani (Core Facility Center, Research Infrastructure Management Center, Institute of Science Tokyo) for his kind assistance with the temperature-modulated SAXS measurements. This work was financially supported by JSPS KAKENHI (Grant Numbers : 20H02785 and 24H00052) and JST SPRING (Grant Number : JPMJSP2106).

REFERENCES

(1) Lecommandoux, S.; Borsali, R.; Schappacher, M.; Deffieux, A.; Narayanan, T.; Rochas, C. Microphase Separation of Linear and

Cyclic Block Copolymers Poly(Styrene-b-Isoprene): SAXS Experiments. *Macromolecules* **2004**, *37* (5), 1843−1848.
(2) Mogi, Y.; Nomura, M.; Kotsuji, H.; Ohnishi, K.; Matsushita, Y.; Noda, I. Superlattice Structures in Morphologies of the ABC Triblock Copolymers. *Macromolecules* **1994**, *27* (23), 6755−6760.
(3) Yoshida, K.; Tanaka, S.; Yamamoto, T.; Tajima, K.; Borsali, R.; Isono, T.; Satoh, T. Chain-End Functionalization with a Saccharide for 10 Nm Microphase Separation: "Classical" PS-b-PMMA versus PS-b-PMMA-Saccharide. *Macromolecules* **2018**, *51* (21), 8870−8877.
(4) Funaki, Y.; Kumano, K.; Nakao, T.; Jinnai, H.; Yoshida, H.; Kimishima, K.; Tsutsumi, K.; Hirokawa, Y.; Hashimoto, T. Influence of Casting Solvents on Microphase-Separated Structures of Poly(2-Vinylpyridine)- Block -Polyisoprene. *Polymer* **1999**, *40* (25), 7147−7156.
(5) Jeong, J. W.; Park, W. I.; Kim, M.-J.; Ross, C. A.; Jung, Y. S. Highly Tunable Self-Assembled Nanostructures from a Poly(2-Vinylpyridine-b-Dimethylsiloxane) Block Copolymer. *Nano Lett.* **2011**, *11* (10), 4095−4101.
(6) Suzuki, M.; Orido, T.; Takano, A.; Matsushita, Y. The Largest Quasicrystalline Tiling with Dodecagonal Symmetry from a Single Pentablock Quarterpolymer of the AB $_1$ CB $_2$ D Type. *ACS Nano* **2022**, *16* (4), 6111−6117.
(7) Lo, T.-Y.; Chao, C.-C.; Ho, R.-M.; Georgopanos, P.; Avgeropoulos, A.; Thomas, E. L. Phase Transitions of Polystyrene-b-Poly(Dimethylsiloxane) in Solvents of Varying Selectivity. *Macromolecules* **2013**, *46* (18), 7513−7524.
(8) Cheng, L.-C.; Bai, W.; Martin, E. F.; Tu, K.-H.; Ntetsikas, K.; Liontos, G.; Avgeropoulos, A.; Ross, C. A. Morphology, Directed Self-Assembly and Pattern Transfer from a High Molecular Weight Polystyrene-Block-Poly(Dimethylsiloxane) Block Copolymer Film. *Nanotechnology* **2017**, *28* (14), 145301.
(9) Matsen, M. W.; Bates, F. S. Unifying Weak- and Strong-Segregation Block Copolymer Theories. *Macromolecules* **1996**, *29* (4), 1091−1098.
(10) Leibler, L. Theory of Microphase Separation in Block Copolymers. *Macromolecules* **1980**, *13* (6), 1602−1617.
(11) Matsen, M. W.; Bates, F. S. Origins of Complex Self-Assembly in Block Copolymers. *Macromolecules* **1996**, *29* (23), 7641−7644.
(12) Jung, Y. S.; Ross, C. A. Orientation-Controlled Self-Assembled Nanolithography Using a Polystyrene−Polydimethylsiloxane Block Copolymer. *Nano Lett.* **2007**, *7* (7), 2046−2050.
(13) Maekawa, S.; Seshimo, T.; Dazai, T.; Sato, K.; Hatakeyama-Sato, K.; Nabae, Y.; Hayakawa, T. Chemically Tailored Block Copolymers for Highly Reliable Sub-10-Nm Patterns by Directed Self-Assembly. *Nat. Commun.* **2024**, *15* (1), 5671.
(14) Zhang, Z.; Gao, L.; Boes, A.; Bajer, B.; Stotz, J.; Apitius, L.; Jakob, F.; Schneider, E. S.; Sperling, E.; Held, M.; Emmler, T.; Schwaneberg, U.; Abetz, V. An Enzymatic Continuous-Flow Reactor Based on a Pore-Size Matching Nano- and Isoporous Block Copolymer Membrane. *Nat. Commun.* **2024**, *15* (1), 3308.
(15) Li, L.; Schulte, L.; Clausen, L. D.; Hansen, K. M.; Jonsson, G. E.; Ndoni, S. Gyroid Nanoporous Membranes with Tunable Permeability. *ACS Nano* **2011**, *5* (10), 7754−7766.
(16) Higuchi, T.; Tajima, A.; Motoyoshi, K.; Yabu, H.; Shimomura, M. Suprapolymer Structures from Nanostructured Polymer Particles. *Angew. Chem., Int. Ed.* **2009**, *48* (28), 5125−5128.
(17) Yabu, H.; Higuchi, T.; Shimomura, M. Unique Phase-Separation Structures of Block-Copolymer Nanoparticles. *Adv. Mater.* **2005**, *17* (17), 2062−2065.
(18) Yang, Y.; Knauss, D. M. Poly(2,6-Dimethyl-1,4-Phenylene Oxide)- *b* -Poly(Vinylbenzyltrimethylammonium) Diblock Copolymers for Highly Conductive Anion Exchange Membranes. *Macromolecules* **2015**, *48* (13), 4471−4480.
(19) Ingratta, M.; Jutemar, E. P.; Jannasch, P. Synthesis, Nanostructures and Properties of Sulfonated Poly(phenylene oxide) Bearing Polyfluorostyrene Side Chains as Proton Conducting Membranes. *Macromolecules* **2011**, *44* (7), 2074−2083.
(20) Rebeck, N. T.; Li, Y.; Knauss, D. M. Poly(Phenylene Oxide) Copolymer Anion Exchange Membranes. *J. Polym. Sci., Part B: Polym. Phys.* **2013**, *51* (24), 1770−1778.
(21) Amiri, S.; Semsarzadeh, M. A.; Amiri, S. Cobalt Mediated Radical Polymerization of 4-Bromo-2, 6-Dimethyl Phenol and Its Copolymerization with Poly (Dimethyl Siloxane) in the Presence of Co(Acac)2: DMF Catalyst. *Silicon* **2019**, *11* (5), 2203−2210.
(22) Tsuchiya, K.; Ohashi, T.; Miyamachi, S.; Osaka, N.; Saito, H.; Ogino, K. Fabrication of Porous Film Based on Poly(2,6-Dimetyl-1,4-Phenylene Ether) Block Copolymer by Supercritical Carbon Dioxide Treatment. *React. Funct. Polym.* **2011**, *71* (9), 958−963.
(23) Semsarzadeh, M. A.; Sh Dadkhah, A.; Sabzevari, A. High-Performance Family of Polymeric Particles Prepared from Poly-(Phenylene Oxide)-Poly(Hexyl Isocyanate) Liquid Crystal Block Copolymer: Synthesis and Properties Study. *Polym. Polym. Compos.* **2022**, *30*, 09673911221104678.
(24) Dmitrenko, M.; Chepeleva, A.; Liamin, V.; Kuzminova, A.; Mazur, A.; Semenov, K.; Penkova, A. Novel PDMS-b-PPO Membranes Modified with Graphene Oxide for Efficient Pervaporation Ethanol Dehydration. *Membranes* **2022**, *12* (9), 832.
(25) Matsen, M. W. Polydispersity-Induced Macrophase Separation in Diblock Copolymer Melts. *Phys. Rev. Lett.* **2007**, *99* (14), 148304.
(26) Mai, Y.; Eisenberg, A. Self-Assembly of Block Copolymers. *Chem. Soc. Rev.* **2012**, *41* (18), 5969.
(27) Lodge, T. P. Block Copolymers: Past Successes and Future Challenges. *Macromol. Chem. Phys.* **2003**, *204* (2), 265−273.
(28) Hay, A. S. Polymerization by Oxidative Coupling: Discovery and Commercialization of PPO® and Noryl® Resins. *J. Polym. Sci., Part A: Polym. Chem.* **1998**, *36* (4), 505−517.
(29) Nunoshige, J.; Akahoshi, H.; Shibasaki, Y.; Ueda, M. Efficient Oxidative Coupling Polymerization for Synthesis of Thermosetting Poly(Phenylene Ether) Copolymer with a Low Dielectric Loss. *J. Polym. Sci., Part A: Polym. Chem.* **2008**, *46* (15), 5278−5282.
(30) Nunoshige, J.; Akahoshi, H.; Ueda, M. Molecular Weight Control of Thermosetting Poly(Phenylene Ether) Copolymer Produced by Heterogeneous Oxidative Coupling Polymerization. *High Perform. Polym.* **2010**, *22* (4), 458−467.
(31) Sinturel, C.; Bates, F. S.; Hillmyer, M. A. High χ−Low N Block Polymers: How Far Can We Go? *ACS Macro Lett.* **2015**, *4* (9), 1044−1050.
(32) Maddani, M. R.; Prabhu, K. R. A Concise Synthesis of Substituted Thiourea Derivatives in Aqueous Medium. *J. Org. Chem.* **2010**, *75* (7), 2327−2332.
(33) Aoyagi, N.; Furusho, Y.; Endo, T. Convenient Synthesis of Acyclic Guanidines from Isothiouronium Iodides and Amines without Protection of the Amino Groups. *Synlett* **2014**, *25* (7), 983−986.
(34) Fuchise, K.; Igarashi, M.; Sato, K.; Shimada, S. Organocatalytic Controlled/Living Ring-Opening Polymerization of Cyclotrisiloxanes Initiated by Water with Strong Organic Base Catalysts. *Chem. Sci.* **2018**, *9* (11), 2879−2891.
(35) Williams, D. B. G.; Lawton, M. Drying of Organic Solvents: Quantitative Evaluation of the Efficiency of Several Desiccants. *J. Org. Chem.* **2010**, *75* (24), 8351−8354.
(36) Fuchise, K.; Kobayashi, T.; Sato, K.; Igarashi, M. Organocatalytic Ring-Opening Polymerization of Cyclotrisiloxanes Using Silanols as Initiators for the Precise Synthesis of Asymmetric Linear Polysiloxanes. *Polym. Chem.* **2020**, *11* (48), 7625−7636.
(37) Lohmeijer, B. G. G.; Dubois, G.; Leibfarth, F.; Pratt, R. C.; Nederberg, F.; Nelson, A.; Waymouth, R. M.; Wade, C.; Hedrick, J. L. Organocatalytic Living Ring-Opening Polymerization of Cyclic Carbosiloxanes. *Org. Lett.* **2006**, *8* (21), 4683−4686.
(38) Hansen, C. M. *Hansen Solubility Parameters: A User's Handbook*, 2nd ed.; CRC Press: Boca Raton, 2007.
(39) Launay, H.; Hansen, C. M.; Almdal, K. Hansen Solubility Parameters for a Carbon Fiber/Epoxy Composite. *Carbon* **2007**, *45* (15), 2859−2865.
(40) Peng, P.; Shi, B.; Jia, L.; Li, B. Relationship between Hansen Solubility Parameters of ABS and Its Homopolymer Components of

https://doi.org/10.1021/acs.macromol.5c00730
Macromolecules 2025, 58, 5271−5282

PAN, PB, and PS. *J. Macromol. Sci., Part B: Phys.* **2010**, *49* (5), 864−869.
(41) Ishizone, T.; Han, S.; Okuyama, S.; Nakahama, S. Synthesis of Water-Soluble Polymethacrylates by Living Anionic Polymerization of Trialkylsilyl-Protected Oligo(Ethylene Glycol) Methacrylates. *Macromolecules* **2003**, *36* (1), 42−49.
(42) Lin, Z.; Nabae, Y.; Hayakawa, T. Control of Microphase-Separated Structures by Tuning the Functional Groups and the Degree of Modification for a Single Block Copolymer. *Polym. Chem.* **2023**, *14* (17), 2045−2053.
(43) Gałka, P.; Kowalonek, J.; Kaczmarek, H. Thermogravimetric Analysis of Thermal Stability of Poly(Methyl Methacrylate) Films Modified with Photoinitiators. *J. Therm. Anal. Calorim.* **2014**, *115* (2), 1387−1394.
(44) Ciolino, A. E.; Villar, M. A.; Vallés, E. M.; Hadjichristidis, N. Synthesis and Characterization of Model Polybutadiene-1,4- *b* -polydimethylsiloxane- *b* -polybutadiene-1,4 Copolymers. *J. Polym. Sci., Part A: Polym. Chem.* **2007**, *45* (13), 2726−2733.
(45) Elmaci, A.; Hacaloglu, J. Thermal Degradation of Poly-(Vinylpyridine)s. *Polym. Degrad. Stab.* **2009**, *94* (4), 738−743.
(46) Wypych, G. PDMS Polydimethylsiloxane. In *Handbook of Polymers* Wypych, G. Ed.; Elsevier: Oxford, 2012; pp. 328−332. DOI: .
(47) Matsen, M. W.; Bates, F. S. Conformationally Asymmetric Block Copolymers. *J. Polym. Sci., Part B: Polym. Phys.* **1997**, *35* (6), 945−952.
(48) Matsen, M. W. Fast and Accurate SCFT Calculations for Periodic Block-Copolymer Morphologies Using the Spectral Method with Anderson Mixing. *Eur. Phys. J. E* **2009**, *30* (4), 361.
(49) Chen, H.-L.; Lu, J.-S.; Yu, C.-H.; Yeh, C.-L.; Jeng, U.-S.; Chen, W.-C. Tetragonally Packed Cylinder Structure via Hierarchical Assembly of Comb−Coil Diblock Copolymer. *Macromolecules* **2007**, *40* (9), 3271−3276.
(50) Chiang, W.-S.; Lin, C.-H.; Yeh, C.-L.; Nandan, B.; Hsu, P.-N.; Lin, C.-W.; Chen, H.-L.; Chen, W.-C. Tetragonally Packed Cylinder Structure of Comb−Coil Block Copolymer Bearing Heteroarm Star Architecture. *Macromolecules* **2009**, *42* (6), 2304−2308.
(51) Kang, S.; Lee, J.; Yoon, H.; Jang, J.; Kim, E.; Kim, J. K. Tetragonally Packed Inverted Cylindrical Microdomains from Binary Block Copolymer Blends with Enhanced Hydrogen Bonding. *ACS Macro Lett.* **2023**, *12* (7), 915−920.
(52) Guliyeva, A.; Vayer, M.; Warmont, F.; Faugère, A. M.; Andreazza, P.; Takano, A.; Matsushita, Y.; Sinturel, C. Thin Films with Perpendicular Tetragonally Packed Rectangular Rods Obtained from Blends of Linear ABC Block Terpolymers. *ACS Macro Lett.* **2018**, *7* (7), 789−794.
(53) Asai, Y.; Yamada, K.; Yamada, M.; Takano, A.; Matsushita, Y. Formation of Tetragonally-Packed Rectangular Cylinders from ABC Block Terpolymer Blends. *ACS Macro Lett.* **2014**, *3* (2), 166−169.

https://doi.org/10.1021/acs.macromol.5c00730
Macromolecules 2025, 58, 5271−5282